Hypertension Research (2019) 42:182–194
https://doi.org/10.1038/s41440-018-0139-9

ARTICLE

Mechanisms of action of *Panax notoginseng* ethanolic extract for its vasodilatory effects and partial characterization of vasoactive compounds

Yean Chun Loh[1] · Chu Shan Tan[1] · Yung Sing Ch'ng[1] · Chiew Hoong Ng[1] · Zhao Qin Yeap[1] · Mun Fei Yam[1]

Received: 28 February 2018 / Revised: 19 May 2018 / Accepted: 24 May 2018 / Published online: 21 November 2018

Abstract

Panax notoginseng is the most valuable medicinal plant and has been used clinically for more than two thousand years to treat various diseases, including hypertension. Previous studies claimed that different isolated compounds from *P. notoginseng* are involved in different pathways for vasodilation. It is strongly believed that these vasodilating compounds might act synergistically in contributing vasodilatory effects via holistic signaling pathways. The present study aims to evaluate the vasodilatory effect and mechanism of action employed by the crude extract of *P. notoginseng*. The fingerprint of *P. notoginseng* was developed using tri-step FTIR and HPTLC. The contents of Rg1 and Rb1 in the active extract (PN95) were further quantified via HPTLC. The vasodilatory effect of PN95 was evaluated using an in vitro aortic ring model. The results showed that PN95 contains a high amount of Rg1 and Rb1, 25.9 and 13.6%, respectively. The vasodilatory effect of PN95 was elicited via the NO/sGC/cGMP and β_2-adrenergic receptors pathways. Furthermore, PN95 could manage vascular tone by regulating action potentials via potassium and both VOCC and IP_3R pathways. The results obtained fulfilled the expected outcome where the PN95 employed more signaling pathways than any of the single active compounds; hence, the holistic therapeutic effect could be achieved and would more easily translate to applications for the treatment of human diseases.

Keywords high-performance thin layer chromatography · Fourier transform infrared · in vitro aortic rings vasodilation · NO/sGC/cGMP · *Panax notoginseng*

Introduction

Hypertension is a major concern in public healthcare, and its variety of concomitant diseases has drawn the attention of scientists to search for higher-efficacy medications from alternative avenues, including the use of traditional Chinese medicine (TCM). TCM mainly relies on the overall observation of symptoms of diseases affecting the human body, which is very different from the reductionistic thinking of Western medicine. TCM has served as an important complimentary alternative medicine since ancient times due to its good therapeutic effects, and it is less likely to give rise to safety concerns. Based on the principles of TCM, hypertension is a multi syndromic disease that can cause phlegm fluid retention, "fire", and deficiency syndromes in the human body. Clinically, there are various kinds of Chinese medicinal herbs that are often used to treat hypertension, among which *Panax notoginseng* is one of the most frequently used and is usually suggested to be taken daily to prevent hypertension [1, 2].

According to the Compendium of Materia Medica, *P. notoginseng* is the most valuable medicinal plant and has been used therapeutically for more than two thousand years [1, 3]. According to traditional beliefs, various properties of *P. notoginseng* can heal all kinds of diseases in the human body [4] by promoting the blood circulation, removing blood stasis without causing "congealed" blood, and inhibiting platelet aggregation [1, 5, 6]. Fundamentally, there are five main types of ginsenosides that constitute up to 90% of total saponins in *P. notoginseng*, including ginsenosides Rg 1 (20–24%), Rb1 (30–36%), Rd (5–8.4%), and

✉ Mun Fei Yam
yammumfei@yahoo.com

[1] Department of Pharmacology, School of Pharmaceutical Sciences, Universiti Sains Malaysia, 11800 Minden, Penang, Malaysia

Re (3.9–6%) and notoginsenoside R1 (7-10%) [7–11]. Previous studies demonstrated that ginsenosides could modulate vascular tone by using different mechanisms. For example, ginsenosides Rb1 and Rg1 are capable of inducing vasodilatory effects by increasing nitric oxide (NO) production in the endothelium [12, 13] with an EC_{50} value of approximately 0.03 mg/ml [12]. Moreover, the NO/soluble guanylyl cyclase (sGC)/cyclic guanosine monophosphate (cGMP) pathways were claimed to be the major routes for ginsenoside Ft1 to elicit endothelium-dependent vasodilatory effects on rat mesenteric arteries with an EC_{50} value of approximately 4.6×10^{-6} M [14]. There were studies that showed that ginsenoside Rd tends to inhibit receptor-operated (ROCC) and store-operated (SOCC) calcium channels but not voltage-operated calcium channels (VOCC) during vascular tone regulation [3, 15, 16].

Furthermore, a few studies suggested that *P. notoginseng* saponin (PNS) is a calcium channel blocker [17] and could induce endothelium-derived relaxation factors such as NO but not prostacyclin (PGI_2) [12]. Interestingly, one study showed that the resulting vasodilatory effect elicited by the *P. notoginseng* crude extract is almost equal to the sum of the effects shown by both ginsenosides Rg1 and Rb1, with an EC_{50} value of approximately 10 mg/ml [10]. Therefore, in the present study, the vasodilatory effects of different crude extracts of *P. notoginseng* were studied to confirm the holistic outcome that has been claimed by TCM. The signaling pathways employed by the most potent *P. notoginseng* extract for eliciting vasodilatory effects were further analyzed by using an in vitro aortic ring model in the presence of antagonists. The fingerprints of the *P. notoginseng* extracts were also developed by using tri-step Fourier transform infrared (FTIR) spectroscopy, and the contents of ginsenosides Rg1 and Rb1 were quantified by using high-performance thin layer chromatography (HPTLC).

Methods

Herbs and chemicals

P. notoginseng was purchased from the local medical hall and physically authenticated by Dr. Yam Mun Fei. Ginsenosides Rg1 and Rb1 were purchased from Chengdu Biopurify Phytochemicals Ltd. (Sichuan, China). The *P. notoginseng* standard herb was purchased from the National Institutes for Food and Drug Control (Beijing, China). Phenylephrine (PE) and acetylcholine (Ach) were purchased from Acros Organics, Belgium. HPTLC 60 G F_{254} plates, potassium bromide (KBr) and 4-aminopyridine (4-AP) were purchased from Merck, Germany. Ethylene glycol tetraacetic acid (EGTA) and methylene blue (MB) were purchased from Promedipharm Sdn. Bhd, Malaysia. Nω-Nitro-L-arginine methyl ester hydrochloride (L-NAME), atropine, propranolol, tetraehtylammonium (TEA), and barium chloride ($BaCl_2$) were purchased from Sigma Aldrich, USA. All the aforementioned chemicals were dissolved by using distilled water, and 2-aminoethoxydiphenyl borate (2-APB), indomethacin, 1H-[1,2,4] oxadiazolo [4,3,-a] quinoxalin-1-one (ODQ), glibenclamide (Sigma Aldrich, USA), and nifedipine (Acros Organics, Belgium) were dissolved by using < % of Tween 80. All the chemicals were kept in the freezer (Pensonic, PFZ-230) at −20 °C.

Crude extracts preparation

The purchased *P. notoginseng* was dried at 50 °C in an oven for 48 h and ground into fine powder. Approximately 200 g of herb powder was weighed and macerated three times in distilled water, 50% ethanol, and 95% ethanol separately at 50 °C for 48 h. After filtration, the filtrate was rotary evaporated at a temperature of up to 50 °C under reduced pressure, and the resultant extracts were freeze-dried. The final yields of distilled water extract (PNW), 50% ethanolic extract (PN50), and 95% ethanolic extract (PN95) of *P. notoginseng* were 10.7, 23.6, and 15.1%, respectively. All the extracts were dissolved by using distilled water and prepared in 64 mg/ml stock solutions and kept in a freezer at −20 °C.

Tri-step FTIR spectroscopy

KBr (100 mg) was pressed into a tablet under the mechanical pressure of 10 psi and was used as a blank before the experiment started. The *P. notoginseng* herb sample was passed through a 200-mesh sieve to obtain a fine powder. Approximately 1 mg of the *P. notoginseng* herb powder and each extract was weighed and mixed evenly with 100 mg of KBr separately. Subsequently, both mixtures were pressed into thin tablets separately under 10 psi (GS15011, Atlas 15 T Manual Hydraulic Press, Specac) and kept in a Petri dish containing desiccants (silica gel). The tablets were separately fixed in transmission sample holders, and their spectra (1D-IR) were recorded at optical path speeds of 0.2 cm/s and 16 coadded scans with 4 cm^{-1} resolution between wavelengths of 400−4000 cm^{-1} by using a Spectrum 400 FT-IR spectrometer (v 6.3.5) equipped with a DTGS detector (Perkin-Elmer, USA). The spectra obtained were considered valid only when at least 60% transmission was achieved. Otherwise, the tablet was reprepared by adding either more KBr or more sample extracts [18].

The second derivative (SD-IR) spectra were obtained by using Savitzky-Golay polynomial fitting with 13-point

smoothing. The 2D-IR spectra were recorded at 10 °C intervals within the temperature range of 50-120 °C, which was controlled by a programmable heated jacket controller (Model GS20730, Specac). Dynamic spectra were obtained by treating the spectra with 2D-IR analysis software developed by Tsinghua University (Beijing, China) [18, 19].

High-performance thin layer chromatography

The ginsenosides Rg1 and Rb1 were prepared at concentrations of 0.25–4 mg/ml by dissolving in methanol. PN95 was prepared in ethanol at 10 and 25 mg/ml. *P. notoginseng* raw and standard herbs were prepared in methanol at 100 mg/ml. All the data were interpreted by using VisionCATs software version 2.2.16187.4 (CAMAG, Muttenz, Switzerland).

Approximately 2 µl of each sample was applied as 8 mm wide bands with an 11.4 mm distance between the bands on 20 × 10 cm HPTLC plates. The bands were applied at a distance of 8 mm from the bottom edge and 20 mm from the left edge. Methanol was used to rinse the spotting needle in three cycles when different samples were applied. The sample-spotted TLC plate was then transferred to ADC 2, which is equipped with 20 × 10 cm of twin-through chambers containing a mobile phase that is made of chloroform/methanol/water (13:8:0.5, v/v/v) at 25 ml for saturation and another 10 ml for development. Before the mobile phase developments, the chamber was saturated for 10 min, and the humidity was maintained at approximately 37%. The mobile phase was allowed to develop up to 70 mm from the bottom edge of the HPTLC plate and was dried for 2 min. The image of the plate was examined using a TLC visualizer at 254 and 366 nm and white light illumination, and the images were captured for further analysis.

A TLC scanner 4 was used to calculate the retardation factor (R_f) values of each band and quantify the contents of the standard compounds. The spectra of ginsenosides Rg1 and Rb1 were scanned at their maximum absorbance unit (AU), 203 nm. The contents of ginsenosides Rg1 and Rb1 in the samples were calculated from the calibration curves of each compound [20]. For derivatization, the plate was dipped into 10% H_2SO_4 reagent by using a TLC immersion device (CAMAG, Muttenz, Switzerland) at a speed of 3.5 cm/s and was heated by using a plate heater (Heidolph, Germany) for 5 min at 105 °C. The derivatized plate was examined in a TLC visualizer, and images were captured for comparison purposes [21].

Animal and aortic rings preparation

Male Sprague Dawley (SD) rats weighing between 180 and 250 g were used throughout the whole experiment ($n = 8$ for each experiment) and acclimated in the animal transit house for 12-h light–dark cycles with free access to food and water at room temperature. The experiment was performed based on the Guideline in Care and Use of Laboratory Animal by Universiti Sains Malaysia (USM/Animal Ethics Approval/ 2016/ (103)/ (774)). Prior to the isolation of the aorta from the SD rats, Krebs-Henseleit (Krebs) solution (4.7 mM KCl, 118.0 mM NaCl, 2.5 mM $CaCl_2$, 25.0 mM $NaHCO_3$, 1.2 mM KH_2PO_4, 11.0 mM glucose, and 1.2 mM $MgSO_4$, pH 7.4) was prepared and continuously aerated with carbogen (5% CO_2 and 95% O_2) in a Petri dish. The SD rats were sacrificed by overdose inhalation of CO_2. The thoracic aorta was immediately isolated and placed in Krebs' solution. After the adipose tissues were removed, the aorta was trimmed into 3–4 mm ring segments and mounted in a tissue bath containing Krebs' solution (10 ml) by using two needle hooks with the temperature maintained at 37 °C and continuous aeration with carbogen gas. One hook was fixed on L-shaped braces, and another hook was connected to the force-electricity transducer (GRASS Force-Displacement Transducer FT03 C Isometric Measurement). The mounted aortic rings were allowed to equilibrate for 45 min, and the Krebs' solution was changed at 15-minute intervals. The resting tension was readjusted to 1.0 g after the change of Krebs' solution. Once the tension of the mounted aortic rings stabilized, the contractile agent, PE (1 µM), and the relaxing agent, Ach (1 µM), were added. The validity of the aortic rings was assured with at least 60% of responses achieved. Then, the aortic rings were rinsed three times with Krebs' solution at 15-minute intervals before PE precontraction.

Vascular response to *P. notoginseng* extracts in PE precontracted aortic rings

The endothelium-intact aortic ring was precontracted with PE (1 µM) for at least 30 min and left until reaching the plateau stage. Then, approximately 100 µl of extracts (PN95, PN50, and PNW) was added into the tissue bath cumulatively from 0.25–32 mg/ml at 20-min intervals. The final concentration of the extracts in a tissue bath containing 10 ml Krebs' solution was 0.6375 mg/ml. The vascular response was detected by a force-electricity transducer and amplified by Quad Bridge amp (AD instrument Australia) and subsequently converted into digital signals by power-Lab 26 T (AD instrument, Australia). The extract (PN95) that elicited the highest vasodilatory effect was further used for mechanistic studies. The concentration-response curve, the half maximal effective concentration (EC_{50}) and the maximum relaxation (R_{max}) value obtained were assigned as controls and compared to different antagonist pretreated groups [22].

Vasodilatory effect of PN95 in endothelium-impaired aortic rings

The intima surface of the isolated aortic rings was removed mechanically by gently rubbing with a stainless steel stick. The integrity of the endothelium-denuded aortic rings was assured by exposure to PE with at least 60% of contraction achieved and no relaxation upon exposure to Ach. The PN95 (0.0025–0.6375 mg/ml) was added to the tissue bath cumulatively at 20-min intervals after PE precontraction.

Vasodilatory effect of PN95 in KCl precontracted aortic rings

The endothelium-intact isolated aortic rings were precontracted with KCl (80 mM). The PN95 (0.0025–0.6375 mg/ml) was then added into the tissue bath cumulatively at 20-min intervals.

Investigation of the roles of EDRFs

The antagonists of endothelial NO synthase (eNOS), L-NAME (10 μM); cyclooxygenase (COX), indomethacin (10 μM); soluble guanylyl cyclase (sGC), ODQ (1 μM); and cyclic guanosine monophosphate (cGMP), MB (10 μM) were preincubated separately with endothelium-intact isolated aortic rings for 20 min before PE precontraction. PN95 (0.0025–0.6375 mg/ml) was then added to the tissue bath cumulatively at 20-min intervals.

Investigation of the roles β_2-adrenergic and muscarinic receptors

The antagonists of β_2-adrenergic, propranolol (1 μM), and muscarinic receptor, atropine (1 μM), were preincubated with endothelium-intact isolated aortic rings separately for 20 min before PE precontraction. PN95 (0.0025-0.6375 mg/ml) was then added to the tissue bath cumulatively at 20-min intervals.

Role of K^+ channels in the vasodilatory effect of PN95

The respective antagonists of ATP-sensitive K^+ channels (K_{ATP}), voltage-activated K^+ channels (K_v), calcium-activated K^+ channels (K_{ca}), and inwardly rectifying K^+ channels (K_{ir}), namely, glibenclamide (10 μM), 4-AP (1 mM), TEA (1 mM), and $BaCl_2$ (10 μM), were added to the tissue bath separately and preincubated with endothelium-intact isolated aortic rings for 20 min before PE precontraction. PN95 (0.0025–0.6375 mg/ml) was then added to the tissue bath cumulatively at 20-min intervals.

Role of VOCC in the vasodilatory effect of PN95

Three sets of experiments were carried out that included positive controls (0.1, 0.3, and 1 μM of nifedipine), experimental groups (0.005, 0.04, and 0.32 mg/ml of PN95), and control sets. The Ca^{2+}-free high K^+ Krebs' solution (11.9 mM $NaHCO_3$, 1.05 mM $MgSO_4$, 91.04 mM NaCl, 50.0 mM KCl, and 5.5 mM glucose, pH 7.4) was used as a buffer solution instead of normal Krebs' solution. Once the integrity of the mounted endothelium-intact aortic rings was validated, the aortic rings were rinsed with normal Krebs' solution three times at 10-minute intervals. Subsequently, the aortic rings were rinsed with EGTA (0.2 mM) that contained Ca^{2+}-free high K^+ Krebs' solution for 10 min to remove the Ca^{2+} residue. Then, the aortic rings were rinsed twice with Ca^{2+}-free high K^+ Krebs' solution at 10-minute intervals. The resting tension was readjusted to 1.0 g if necessary. In the control set, $CaCl_2$ was added to the tissue bath cumulatively (0.01–10 mM) at 3-minute intervals. In the positive control set, the selective antagonist of VOCC, nifedipine (0.1, 0.3, and 1 μM) was added to the tissue bath and incubated for 20 min before the cumulative addition of $CaCl_2$. In the experimental sets, PN95 (0.005, 0.04, and 0.32 mg/ml) was used for preincubation. After that, concentration-response curves were constructed, and the maximum contraction tension (C_{max}) values were recorded and compared to each other [23–25].

Role of IP_3R in the vasodilatory effect of PN95

Three sets of experiments were carried out, including positive controls (100 μM of 2-APB), experimental groups (0.005, 0.04, and 0.32 mg/ml of PN95), and control sets. A similar protocol as described in the VOCC mechanistic study was utilized. The only different step from the VOCC protocol was that cumulative addition of $CaCl_2$ was replaced by adding PE (1 μM) and left for 20 min to induce transient contraction. 2-APB and PN95 (0.005, 0.04, and 0.32 mg/ml) were preincubated with the endothelium-denuded isolated aortic rings for 20 min before the addition of PE for the positive control and experimental sets, respectively. The C_{max} values were recorded and compared [23–25].

Statistical analysis

All the data were expressed as the mean ± S.E.M. The results obtained for antagonist pretreated groups were compared to the control by using one-way ANOVA and post hoc Dunnett's test with the use of SPSS version 22 software. All tests were two-tailed, and the significance rejection value was fixed at $P < 0.05$.

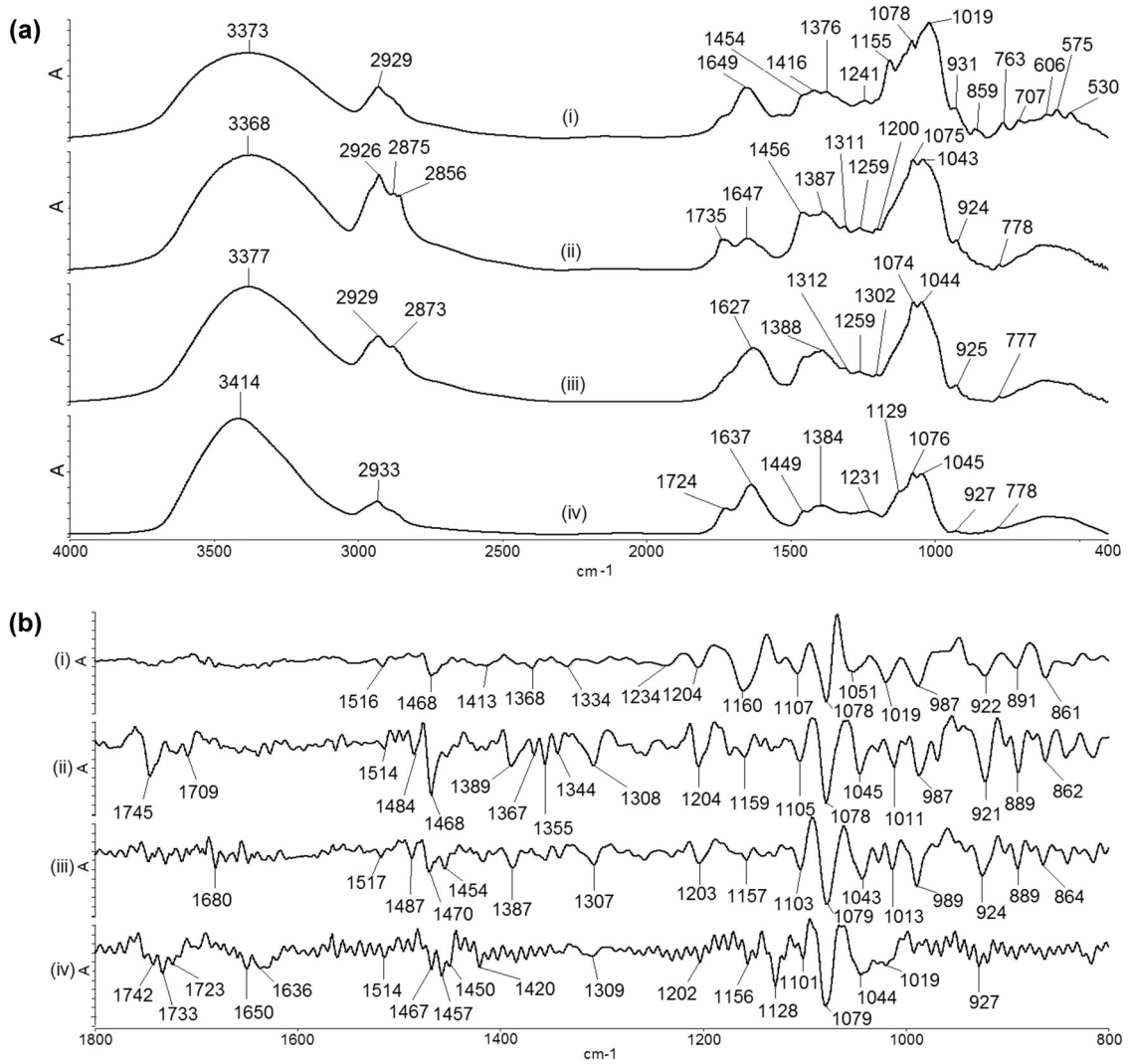

Fig. 1 Representative **a** 1D-IR spectra in the range of 400–4000 cm^{-1} and **b** SD-IR spectra in the range of 800–1800 cm^{-1} for (i) raw powder of *P. notoginseng;* (ii) 95% ethanolic *P. notoginseng* extract (PN95); (iii) 50% ethanolic *P. notoginseng* extract (PN50); and (iv) distilled water *P. notoginseng* extract (PNW)

Results

Tri-step IR macrofingerprint analysis of *P. notoginseng* herb and its extracts

According to Fig. 1a (i), the spectrum of *P. notoginseng* herb powder is exactly the same as the spectra shown in the atlas established by Sun et al. [26]. The characteristic peaks of powdered *P. notoginseng* and its extract, as shown in Fig. 1a (ii), (iii), and (iv), are tabulated in Table 1, and their SD-IR spectra [27] are shown in Fig. 1b (i), (ii), (iii), and (iv). The dynamic spectra of *P. notoginseng*, PN95, PN50, and PNW were further analyzed [28] and expressed in two different ranges of approximately 800–1150 cm^{-1} and 1100–1800 cm^{-1} for autopeaks. The 2D-IR and 3D-IR spectra are shown in Fig. 2 and Fig. 3, respectively. The range of wavelength selected varies based on the visibility of the peak's pattern of each extract. For instance, the ranges selected for powdered *P. notoginseng* were 850–1150 cm^{-1} (Fig. 2a) and 1150–1800 cm^{-1} (Fig. 3a). The ranges selected for PN95 were 800–1100 cm^{-1} (Fig. 2b) and 1100–1800 cm^{-1} (Fig. 3b), and for PN50, the ranges selected were 900–1150 cm^{-1} (Fig. 2c) and 1150–1800 cm^{-1} (Fig. 3c). The ranges chosen for the PNW were 850–1150 cm^{-1} (Fig. 2d) and 1200–1800 cm^{-1} (Fig. 3d).

High-performance thin-layer chromatography

According to Fig. 4a–c, the derivatized TLC plate was examined under ultraviolet light at 366 nm, 254 nm, and white light, respectively. The R_f values of both the identity compounds, ginsenoside Rg1 and Rb1, were obtained at 0.697 and 0.129, respectively. These bands appeared in

Table 1 The FTIR spectra peak characterization of raw powder, 95% ethanolic (PN95), 50% ethanolic (PN50), and water extracts (PNW) of *Panax notoginseng*

Peak (cm^{-1})				Primary structure	Possible compounds
Raw	PN95	PN50	PNW		
3373	3368	3377	3414	O-H, ν	Various
2929	2926	2929	2933	C-H, ν_{as}	-
	2875	2873		C-H, ν_s	-
	2856			C-H, ν_s	-
	1735		1724	C=O, ν	Ester
1649	1647			O-H, δ	Glycoside
		1627	1637	Ring	Aromatic
1454	1456		1449	Ring	Aromatic
1416				(O) C-H, δ	Saccharides
1376	1387	1388	1384	NO_2^-, ν_s	Nitrite
	1311	1312		(O) C-H, δ	Saccharides
	1259	1259		C-O, ν	Various
1241			1231	C-O, ν	Ester, Glycoside
	1200	1202		C-O, ν	Saccharides
1155			1129	C-O, ν	Saccharides
1078	1075	1074	1076	C-O, ν	Saccharides
	1043	1044	1045	C-O, ν	Saccharides
1019				C-O, ν	Saccharides

raw purchased *P. notoginseng* raw herb, *PN95* 95% ethanolic extract of *P. notoginseng, PN50* 50% ethanolic extract of *P. notoginseng, PNW* water extract of *P. notoginseng*, ν stretching, ν_s symmetrical stretching, ν_{as} asymmetrical stretching, δ bending

PN95, *P. notoginseng* raw herb, and standard herbs at similar R_f values (Table 2). Therefore, the authenticity of the raw materials used throughout the whole study was strongly verified. Furthermore, the results showed that PN95 contained 25.9 and 13.6% Rg1 and Rb1, respectively.

Vasodilatory effect of *P. notoginseng* extracts

From the preliminary examination, PN95 exerted the highest vasodilatory effect compared to PNW and PN50 until the final concentration of 0.6375 mg/ml in the tissue bath, with the lowest EC_{50} value and highest R_{max} values, as shown in Table 3. Hence, PN95 was further analyzed for its potential signaling pathways employed for vasodilatory activity.

Endothelium and channel-linked receptor dependency

According to Fig. 5 and Table 3, the vasodilatory effect induced by PN95 on the PE precontracted aortic rings was significantly attenuated in the absence of endothelium with an approximately 80% increase in the EC_{50} value ($P < 0.01$, $n = 8$) compared to endothelium-intact samples. However, the R_{max} value decreased when the final concentration of PN95 was applied. Furthermore, the vasodilatory effect elicited by PN95 on KCl precontracted aortic rings shows a dramatic decrease of approximately 23% of the R_{max} value compared to control, whereas the EC_{50} value was significantly increased ($P < 0.001$, $n = 8$).

Role of eNOS/sGC/cGMP

According to Fig. 6 and Table 3, the presence of L-NAME, sGC, and MB crucially diminished the vasodilatory activity of PN95 compared to the control. Down the signaling cascade, the inhibitory effect of the antagonists on the PN95 vasodilatory effect could be arranged in an ascending manner as MB<L-NAME<ODQ, whereas the presence of indomethacin did not affect the vasodilatory activity induced by PN95.

Role of G-protein-coupled muscarinic- and β_2-adrenergic receptors

According to Fig. 7, the maximum vasodilatory effect of PN95 was abundantly suppressed by up to 28% in the presence of propranolol, and there was an approximately threefold increase in the EC_{50} value ($P < 0.001$, $n = 8$) compared to the control, as shown in Table 3. Furthermore, the presence of atropine did not inhibit the vasodilatory effect elicited by PN95 in endothelium-intact isolated aortic rings.

Role of potassium channels

The presence of glibenclamide significantly attenuated the hyperpolarization current induced by PN95 and caused the EC_{50} value to increase up to 0.549 ± 0.099 mg/ml ($P < 0.001$, $n = 8$), which was approximately 12-fold higher than the value of the control. The presence of $BaCl_2$ significantly reduced the vasodilatory effect of PN95 compared to control, which produced an EC_{50} value of 0.132 ± 0.018 mg/ml ($P < 0.001$, $n = 8$). In addition, the presence of 4-AP mildly suppressed the vasodilatory effect of PN95 beginning from the cumulative concentration of 0.0375 mg/ml, which resulted in an EC_{50} value of 0.104 ± 0.046 mg/ml ($P < 0.05$, $n = 8$). It is apparent that the concentration-response curve of PN95 in the presence of 4-AP shifted to the right, as shown in Fig. 8, which implied that the antagonizing effect of 4-AP was time-dependent. Furthermore, the vasodilatory effect induced by PN95 in the presence of TEA was significantly different from that of the control, for which the EC_{50} value was 0.032 ± 0.004 mg/ml ($P < 0.05$, $n = 8$). The R_{max} and EC_{50} values are shown in Table 3.

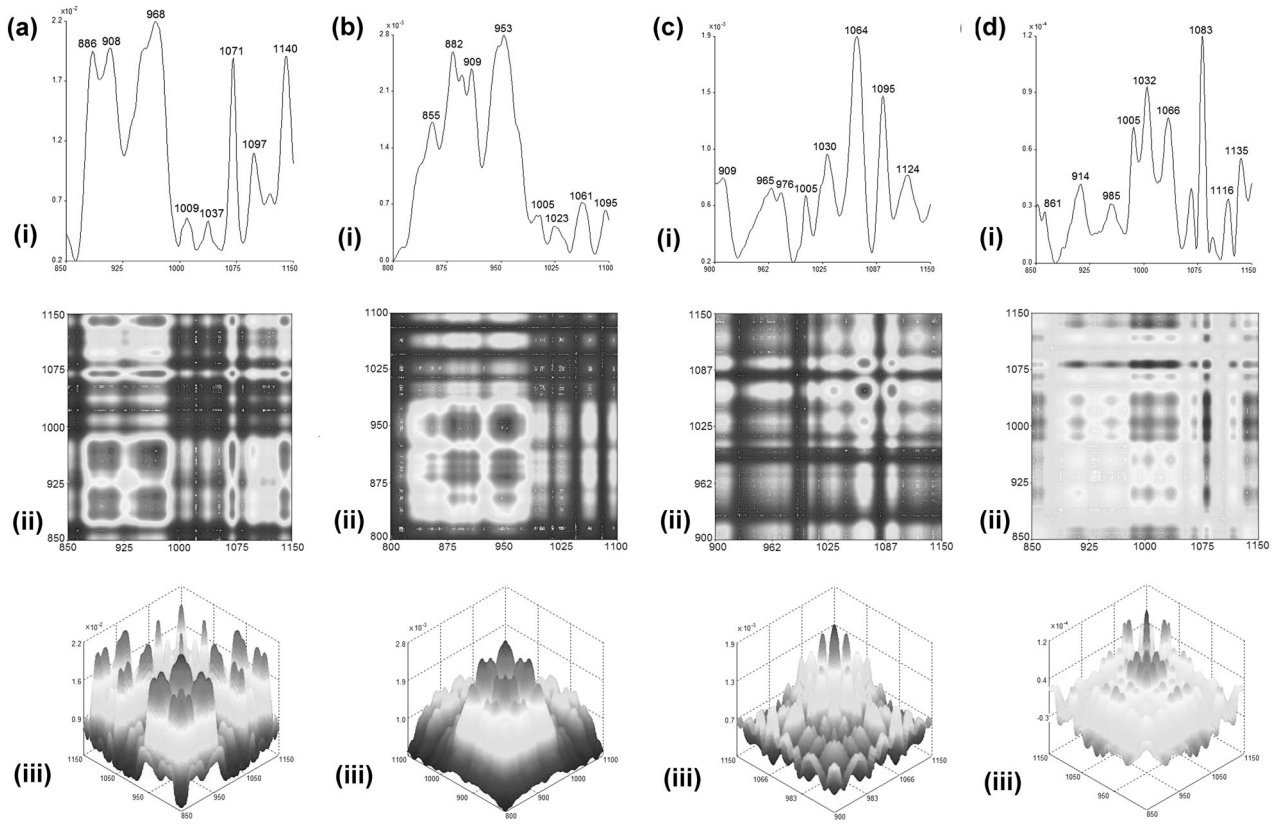

Fig. 2 Representative (i) autopeak, (ii) synchronous 2D-IR, and their (iii) 3D-IR spectra in the range of approximately 800–1150 cm^{-1} for **a** raw powder of *P. notoginseng*; **b** 95% ethanolic *P. notoginseng* extract (PN95); **c** 50% ethanolic *P. notoginseng* extract (PN50); and **d** distilled water *P. notoginseng* extract (PNW)

Role of calcium channels

In the control sets, the C_{max} values obtained for the VOCC and IP_3R mechanistic studies were 0.700 ± 0.032 and 0.719 ± 0.057 g, respectively, as shown in Table 4. In the positive control sets, the maximum contraction induced by the cumulative addition of $CaCl_2$ (0.01–10 mM) to the endothelium-intact isolated aortic rings was almost abolished ($P < 0.001$, $n = 8$) in the presence of nifedipine (in a concentration-dependent manner) or 2-APB compared to control, as shown in Fig. 9a, b, respectively, proving the reliability of both experimental protocols. In terms of the VOCC and IP_3R experimental studies, a high concentration (0.32 mg/ml) of PN95 dramatically attenuated ($P < 0.001$, $n = 8$) the C_{max} values in both mechanistic pathways, with approximately 50% and 62% of the maximum contraction tension suppressed compared to their respective controls, as shown in Table 4. Similarly, both 0.04 and 0.32 mg/ml PN95 significantly blocked the depolarizing current of the membrane potential induced by the calcium influx via VOCC; hence, the C_{max} values obtained were dramatically reduced ($P < 0.001$, $n = 8$) compared to those of the control, as shown in Fig. 9a. However, 0.04 mg/ml PN95 only moderately significantly ($P < 0.01$, $n = 8$) prevented calcium release via the IP_3R, whereas 0.005 mg/ml PN95 did not produce any effect in terms of blocking the IP_3R pathway, as shown in Fig. 9b. Apparently, in the VOCC experimental studies where the endothelium-intact isolated aortic rings were preincubated with PN95 (0.005, 0.04, and 0.32 mg/ml), the contraction tension induced by the cumulative addition of $CaCl_2$ started to decline at a concentration of 3 mM, as shown in Fig. 9a. In addition, the antagonizing effects of PN95 in both VOCC and IP_3R were less than that of the positive control in a concentration-dependent manner.

Discussion

Before the commencement of the experiments, the purchased *P. notoginseng* raw herb was authenticated by using tri-step FTIR spectroscopy [26]. As mentioned above, PN95 elicited the highest vasodilatory effect compared to PNW and PN50; hence, the spectra were analyzed, and peak characteristics were compared. Generally, the ginsenosides are unique components present in all genera of *Panax* that play crucial roles in most pharmacological effects to counteract a variety of diseases [14, 29].

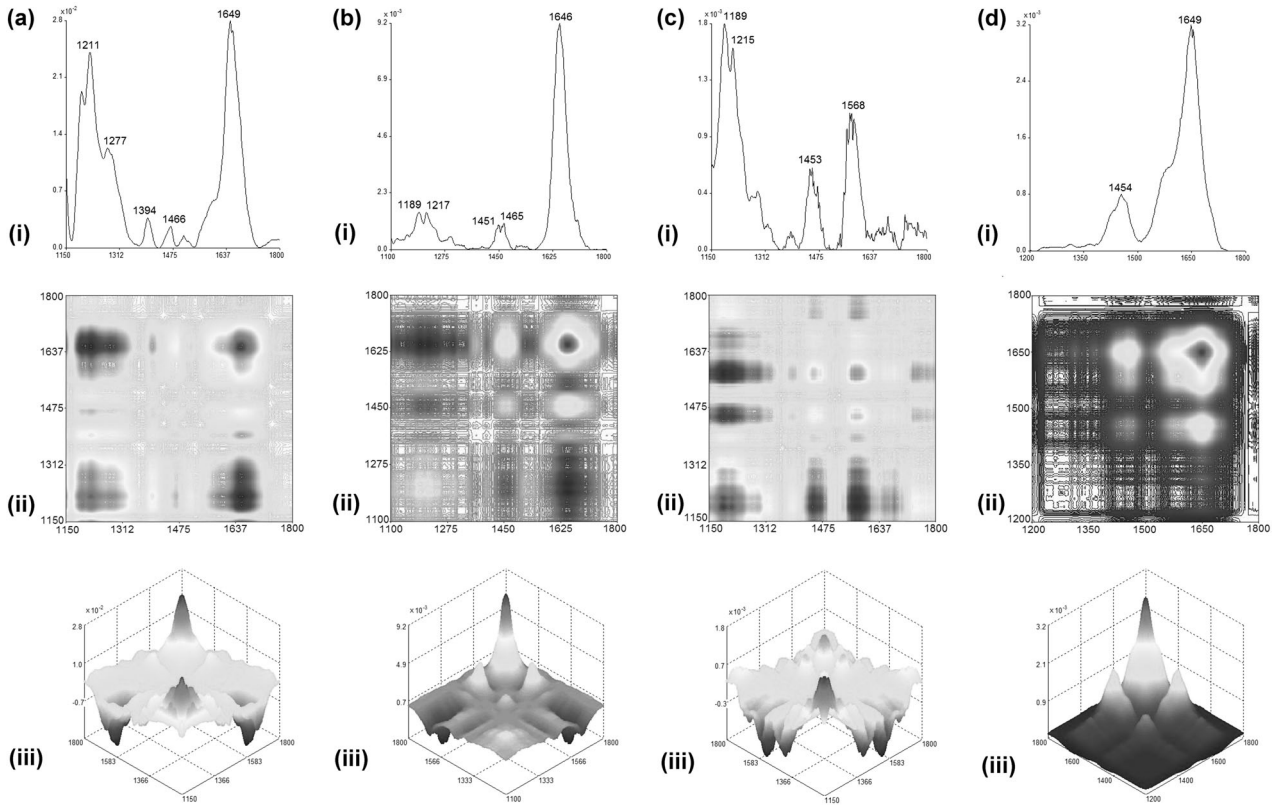

Fig. 3 Representative (i) autopeak, (ii) synchronous 2D-IR, and their (iii) 3D-IR spectra in the range of approximately 1100–1800 cm^{-1} for **a** raw powder of *P. notoginseng*; **b** 95% ethanolic *P. notoginseng* extract (PN95); **c** 50% ethanolic *P. notoginseng* extract (PN50); and **d** distilled water *P. notoginseng* extract (PNW)

The results showed that the main differences between PN95's 1D-IR spectrum and those of other extracts were the peaks that appeared at 2875, 2856, 1735, and 1456 cm^{-1}, which represented symmetrical methyl C-H, methylene C-H bond, carbonyl C=O stretching modes and a methyl C-H bending mode, respectively, indicating that the contents of ester group compounds were higher in PN95 than in the other two extracts. A unique peak appeared at approximately 1647 cm^{-1}, denoting the presence of ginsenosides. Although the characteristic peaks of saponins appeared at approximately 1159 and 1078 cm^{-1} in the SD-IR spectra of all three extracts [30], the peaks that appeared at 1709 cm^{-1} (C=O stretching), 1627 cm^{-1}, 1514 cm^{-1}, 1484 cm^{-1} (aromatic ring skeleton vibration) and 1468 cm^{-1} (C-H bending) in the SD-IR spectrum of PN95 were sharper than those of the other two extracts, which means there was a higher content of flavonoids in PN95.

In the 2D-IR spectrum of *P. notoginseng* raw powder and PN95, the autopeaks that appeared in the range of 850–1000 cm^{-1} indicated the presence of aromatic compounds that could have belonged to ginsenosides, further enforcing its contributions to the vasodilatory effect. In the range of approximately 1100–1800 cm^{-1}, there was a sharp autopeak that appeared at approximately 1650 cm^{-1}, which is the characteristic peak of the O-H bond of glycosides. Interestingly, the 2D-IR spectra of both PN95 and PNW contained this peak, which means that both compounds consisted of glycosides that could act as ginsenosides. As mentioned above, PN95 also contained aromatic rings that belong to ginsenosides. Since PN95 contained a larger amount of ginsenosides than did PNW and PN50, it produced the strongest vasodilatory effect on the vasculature.

In addition, the bands that appeared on the HPTLC plate for both raw and standard herbs were identical, thus proving that these samples are authentic. PN95 claimed to exhibit the strongest vasodilatory effect compared to PN50 and PNW; thus, the contents of the identity compounds of *P. notoginseng*, ginsenosides Rg1 and Rb1, in PN95 were quantified [7, 9]. Apparently, there was 25.9% ginsenoside Rg1 in PN95, which reached the maximum extractable value of Rg1 in *P. notoginseng* (20–24%). There was 13.6% Rb1 in PN95, which is almost half the maximum extractable value of Rb1 in *P. notoginseng* (30–36%) [7–11]. The high contents of both Rg1 and Rb1 could be the key for PN95 to elicit a stronger vasodilatory effect than the others.

In regards to the mechanistic studies, isolated aortic rings were used in vitro to determine the signaling mechanisms

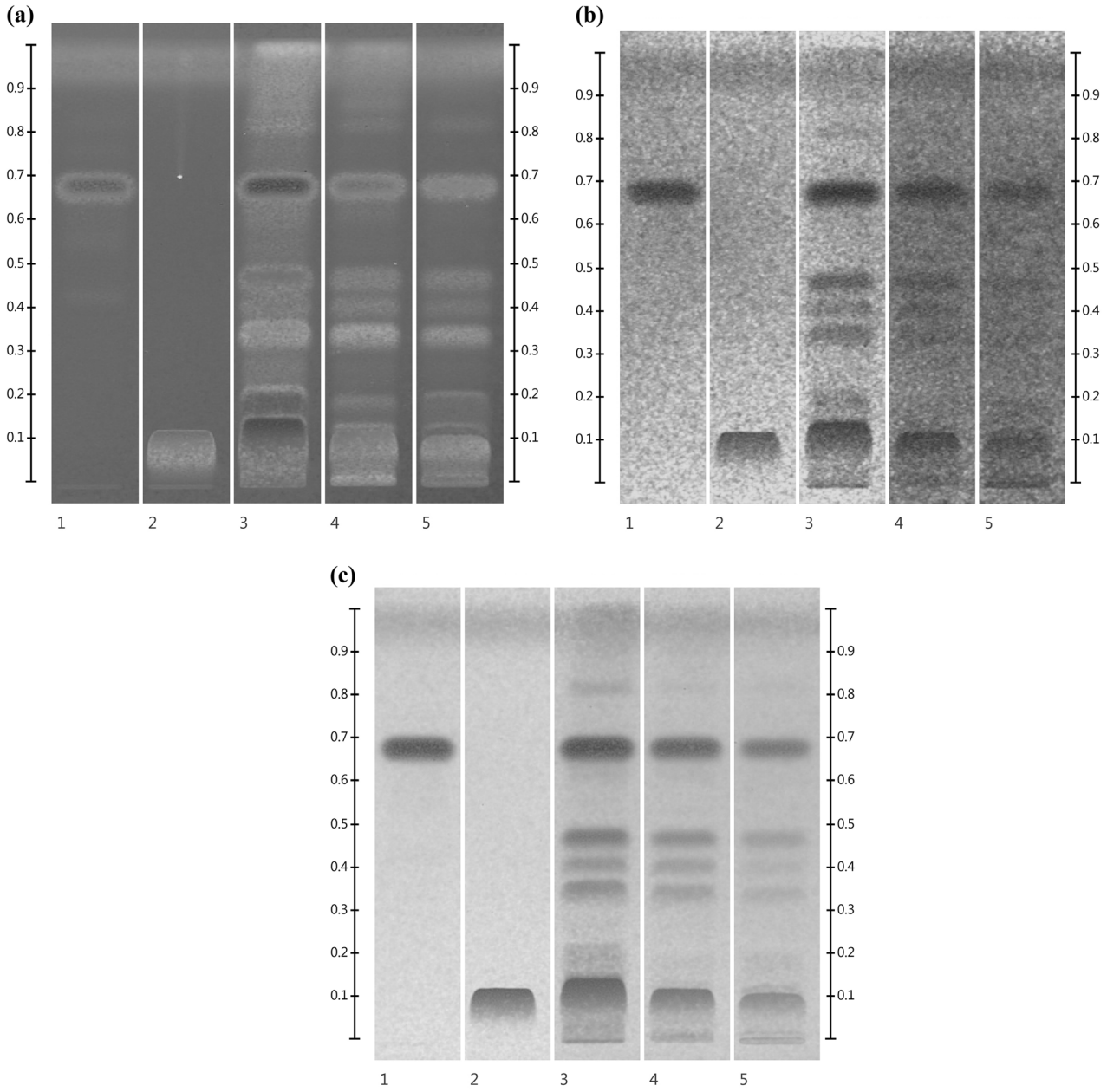

Fig. 4 **a** The HPTLC plate examined under ultraviolet light at 366 nm for ginsenoside Rg 1 (track 1), ginsenoside Rb 1 (track 2), 95% ethanolic *P. notoginseng* extract (track 3), *P. notoginseng* standard herb (track 4) and *P. notoginseng* raw herb (track 5), with a retardation factor (R_f) tool provided at both sides. **b** The HPTLC plate examined under ultraviolet light at 254 nm for ginsenoside Rg 1 (track 1), ginsenoside Rb 1 (track 2), 95% ethanolic *P. notoginseng* extract (track 3), *P. notoginseng* standard herb (track 4) and *P. notoginseng* raw herb (track 5), with a retardation factor (R_f) tool provided at both sides. **c** The HPTLC plate examined under white light for ginsenoside Rg 1 (track 1), ginsenoside Rb 1 (track 2), 95% ethanolic *P. notoginseng* extract (track 3), *P. notoginseng* standard herb (track 4) and *P. notoginseng* raw herb (track 5), with a retardation factor (R_f) tool provided at both sides

employed by PN95 vasodilatory effects since this method is the "gold standard" in pharmacological research on vasculature [23, 31]. According to the results obtained, PN95 could elicit the production of NO by enhancing the activity of eNOS in the vasculature, whereas COX did not play any role in the PN95 vasodilatory effect. These findings were consistent with those of previous publications [11–14, 32–34]. Down the NO-signaling cascade, both sGC and cGMP are found to be involved in the PN95 vasodilatory effect, which is again similar to previous findings [12, 14]. In addition to this finding, the antagonists ODQ and MB were used to further differentiate the cGMP dependency of PN95's vasodilatory effect; this step was not performed in any previous studies [35, 36]. Interestingly, the results proved that sGC, the NO receptor, was the major vasodilator component evoked by PN95 during its

Table 2 Summary of qualitative and quantitative analysis of ginsenosides Rg1 and Rb1 on 95% ethanolic extract, raw herb, and standard herb of *Panax notoginseng* by using HPTLC identification method

Parameter	Ginsenoside Rg1			Ginsenoside Rb1		
	PN95	Raw herb	Standard herb	PN95	Raw herb	Standard herb
Regression mode	Linear-2			Linear-2		
Linear calibration curve	$y = 8.773 \times 10^{-10}x\text{-}2.93 \times 10^{-3}$			$y = 6.432 \times 10^{-10}x\text{-}2.106 \times 10^{-3}$		
R	0.999817			0.869726		
Identity compound linearity range (mg/ml)	0.25–4			2-4		
Identity compound contents (mg/ml)	2.590 ± 0.002	2.398	2.449	3.416 ± 0.188	2.379	3.331
R_f	0.684	0.676	0.681	0.137	0.098	0.111

PN95 95% ethanolic extract of *P. notoginseng*, *raw herb* purchased *P. notoginseng* raw herb, *standard herb P. notoginseng* standard herb purchased from National Institutes for Food and Drug Control, China, *R* correlation coefficient, R_f retardation factor

Table 3 Significance of EC_{50} values and comparison of R_{max} values among different pre-treatments

Treatments	EC_{50} values (mg/ml)	R_{max} values (%)
First line screening		
Control	0.043 ± 0.007	110.19 ± 2.04
KCl	0.331 ± 0.065[a]	84.91 ± 3.64
Denuded	0.078 ± 0.014[b]	106.49 ± 3.97
EDRFs and NO cascade mechanisms		
L-NAME	0.085 ± 0.014[a]	100.66 ± 3.11
ODQ	0.759 ± 0.236[a]	62.88 ± 4.51
MB	0.073 ± 0.012[b]	99.02 ± 3.84
Indomethacin	0.031 ± 0.003	109.59 ± 1.58
GPCRs		
Atropine	0.036 ± 0.003	105.40 ± 2.40
Propanolol	0.162 ± 0.049[a]	79.18 ± 4.04
Potassium channel-linked receptors		
TEA	0.032 ± 0.004[c]	119.47 ± 3.71
Glibenclamide	0.549 ± 0.099[a]	70.46 ± 5.54
4-AP	0.104 ± 0.046[c]	107.89 ± 5.46
$BaCl_2$	0.132 ± 0.018[a]	90.19 ± 1.64

EC_{50} half of effective concentration, *EDRFs* endothelium-derived relaxing factors, *GPCRs* G-protein-coupled receptors, R_{max} maximal relaxation, *n* number of determination

[a]Significance $P < 0.001$

[b]Significance $P < 0.01$

[c]Significance $P < 0.05$

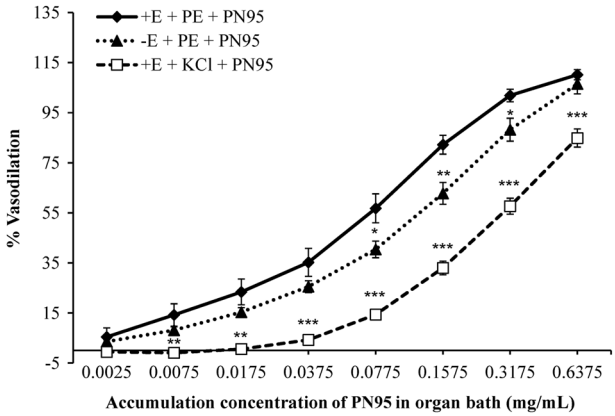

Fig. 5 The cumulative concentration-response curves of the vasodilatory effect elicited by 95% ethanolic *P. notoginseng* extract (PN95) on PE-precontracted endothelium-intact (+E), endothelium-denuded (−E), or KCl-precontracted isolated endothelium-intact rat aortic rings. The cumulative concentration-response curve of PN95 in endothelium-intact aortic rings was assigned as a control. Significant reduction of PN95 vasodilatory effects in both endothelium-denuded and KCl-primed aortic rings (*$P < 0.05$; **$P < 0.01$; ***$P < 0.001$; $n = 8$)

activation down the endothelium-derived NO signaling cascade.

In terms of an endothelium-independent relaxation factor, the present findings showed that PN95 could activate AC by reacting with the β_2-adrenergic receptor, hence upregulating the production of the second messenger, cAMP, and evoking the activation of PKA to achieve a vasodilatory effect [37]. The involvement of the $G_q\alpha$-protein-coupled muscarinic receptor that was functionally predominant in the vascular endothelium during the vasodilatory effect of PN95 was excluded. In the vasculature, both mechanistic pathways played pivotal roles in vascular tone regulation but were not investigated in any previous publications. Therefore, the present study provided additional information that the endothelium-independent β_2-adrenergic receptor was playing a role in the vasodilatory effect of PN95. Furthermore, the β_2-adrenergic receptor was considered the main mechanistic pathway employed by PN95 to evoke the production of cAMP and activate PKA in VSMC to achieve a vasodilatory effect because the reaction of PGI_2 on the prostacyclin receptor (IP) was excluded.

Regarding the channel-linked receptors, four major potassium channels that functionally dominated in regulating action potentials of VSMC were investigated and found

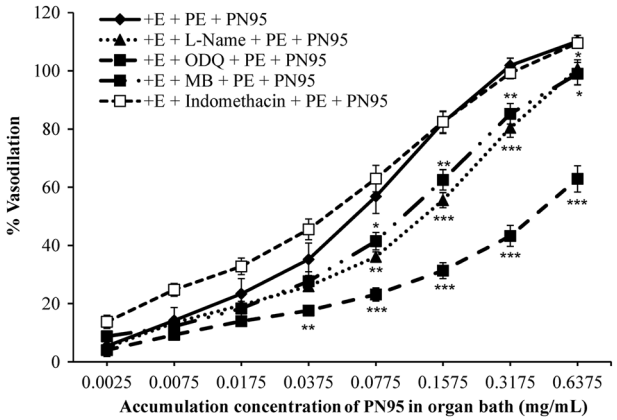

Fig. 6 The cumulative concentration-response curves of vasodilatory effect elicited by 95% ethanolic *P. notoginseng* extract (PN95) in the presence of L-NAME, ODQ, MB, or indomethacin on PE-precontracted isolated endothelium-intact (+E) aortic rings. All antagonists significantly inhibited PN95's vasodilatory effects except indomethacin (*$P < 0.05$; **$P < 0.01$; ***$P < 0.001$; $n = 8$)

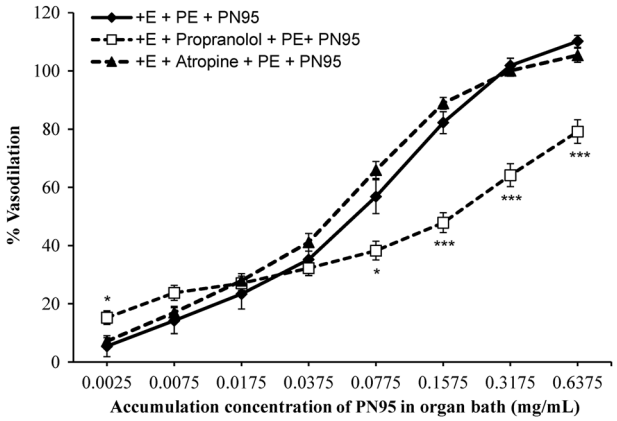

Fig. 7 The cumulative concentration-response curves of the vasodilatory effect elicited by 95% ethanolic *P. notoginseng* extract (PN95) in the presence of atropine or propranolol on PE-precontracted isolated endothelium-intact (+E) aortic rings. Significant decrease in PN95's vasodilatory effects in the presence of propranolol but not atropine (*$P < 0.05$; ***$P < 0.001$; $n = 8$)

to be significant in PN95's vasodilatory effect [38, 39]. The present findings showed similar outcomes to those reported in previous publications. Furthermore, the present findings demonstrated that the K_{ATP} channel was predominant in hyperpolarizing the membrane potential of VSMCs by allowing the K^+ ions to efflux from the cytosol, followed by K_{ev} and K_{ca} channels. In addition, PN95 was capable of expediting the action potential back to the basal stage by using the K_{ir} channel. Therefore, the extent of the potassium channels employed by PN95 could be arranged in ascending order as follows: $K_{ca} < K_v < K_{ir} < K_{ATP}$ channels. In the endothelium, PN95 could act as a K^+ ion channel opener and induce the endothelium-derived hyperpolarizing factor (EDHF) to cause vasodilation [40, 41]. The concentration-response curves obtained in the presence of potassium

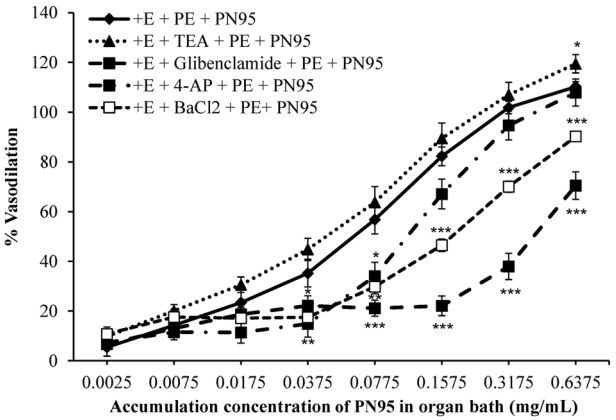

Fig. 8 The cumulative concentration-response curves of the vasodilatory effect elicited by 95% ethanolic *P. notoginseng* extract (PN95) in the presence of TEA, glibenclamide, 4-AP, or $BaCl_2$ on PE-precontracted isolated endothelium-intact (+E) aortic rings. All antagonists significantly inhibited PN95's vasodilatory effects (*$P < 0.05$; **$P < 0.01$; ***$P < 0.001$; $n = 8$)

Table 4 Comparison of C_{max} values among different treatments on calcium channels mechanism studies

Treatments	C_{max} values (g)
VOCC	
Control	0.700 ± 0.032
0.1 μM Nif	0.155 ± 0.010[a]
0.3 μM Nif	0.108 ± 0.008[a]
1 μM Nif	0.049 ± 0.007[a]
0.005 mg/ml PN95	0.501 ± 0.028[a]
0.04 mg/ml PN95	0.409 ± 0.026[a]
0.32 mg/ml PN95	0.354 ± 0.026[a]
IP_3R	
Control	0.719 ± 0.057
100 μM 2-APB	0.024 ± 0.009[a]
0.005 mg/ml PN95	0.684 ± 0.030
0.04 mg/ml PN95	0.386 ± 0.044[b]
0.32 mg/ml PN95	0.280 ± 0.031[a]

2-APB 2-aminoethoxydiphenyl borate, *C_{max}* maximal contraction, PN95, 95% ethanolic extract of *P. notoginseng*, *IP_3R* inositol triphosphate receptor, *Nif* nifedipine, *VOCC* voltage-operated calcium channel

[a]Significance $P < 0.001$;

[b]Significance $P < 0.01$

channel antagonists shifted to the right, indicating the competitive binding site among the antagonists and PN95.

Previous findings claimed that VOCC was ruled out in the mechanistic pathways employed for the vasodilatory effect elicited by ginsenoside Rd, which is one of the chemical constituents within *P. notoginseng* [3, 15, 16]. However, the present findings demonstrated that PN95 could act as a blocker for both VOCC and IP_3R to avoid Ca^{2+} ion influx-induced membrane depolarization, thus

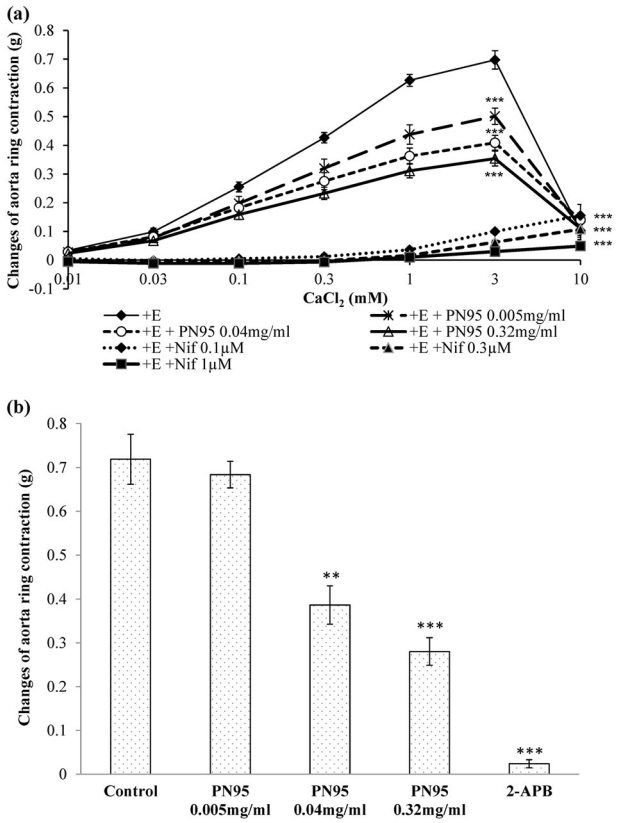

Fig. 9 Effect of different concentrations of 95% ethanolic *P. notoginseng* extract (PN95) (0.005, 0.04, 0.32 mg/ml) and nifedipine (0.1, 0.3, 1 μM) on $CaCl_2$-induced contraction in endothelium-intact (+E) isolated aortic rings in Ca^{2+}-free Krebs' solution. **a** shows that nifedipine almost abolished the $CaCl_2$-induced contraction, whereas all concentrations of PN95 significantly inhibited the $CaCl_2$-induced contraction but to a lesser extent than nifedipine (***$P < 0.001$; $n = 8$). Effects of different concentrations of 95% ethanolic *P. notoginseng* extract (PN95) (0.005, 0.04, 0.32 mg/ml) and 2-APB on PE-induced contraction from intracellular Ca^{2+} release in isolated endothelium-denuded aortic rings in Ca^{2+}-free Krebs' solution. **b** shows that PN95 and 2-APB were significantly inhibited PE-induced contraction from intracellular Ca^{2+} release through IP_3R (**$P < 0.01$; ***$P < 0.001$; $n = 8$)

reducing the formation of calcium-calmodulin complexes, deactivating the myosin-light-chain kinase (MLCK), resulting in the relaxation of VSMCs [42]. These phenomena could happen because PN95 is a crude extract that contains various kinds of chemical components, which could act in multiple mechanistic pathways. Moreover, the plots showed that the addition of 10 mM $CaCl_2$ to the PN95 preincubated aortic rings caused a decrease in the tone of the contraction tension (Fig. 9a), which could be due to the aortic rings reaching their maximum depolarization tone, and a subsequently return to the repolarization state in which the aortic rings start to relax. Furthermore, both VOCC and K_v channels were found to be significant in eliciting the vasodilatory effect of PN95; this fact could be explained by the fact that both channels are functionally correlated in regulating the membrane potential of VSMCs. According to the results shown, the antagonizing effect elicited by PN95 in both receptors was concentration-dependent and occurred to a lesser extent compared to their respective positive controls.

Conclusions

Generally, PN95 was found to contain higher quantities of ginsenosides Rg1 and Rb1 than PN50 or PNW. The signaling pathways involved were proven to be dominated by the NO/sGC/cGMP pathway, followed by the β_2-adrenergic receptor-mediated AC/cAMP pathway. PN95 could further act as a K^+ opener in both the endothelium (EDHF) and VSMCs and to act as a blocker for both the VOCC and IP_3R pathways in regulating the action potential of vascular tone. The present findings demonstrated that the crude extract of *P. notoginseng* could antagonize more vasoconstriction-mediated signaling pathways than any of the fractionated single compounds of *P. notoginseng*, with an EC_{50} value of 0.043 ± 0.007 mg/ml.

Acknowledgements We are grateful for the contributions of all the coauthors and the comments of the reviewers of this manuscript.

Compliance with ethical standards

Conflict of interest The authors declare no conflicts of interest.

References

1. Yang BR, Cheung KK, Zhou X, Xie RF, Cheng PP, Wu S et al. Amelioration of acute myocardial infarction by saponins from flower buds of *Panax notoginseng* via pro-angiogenesis and anti-apoptosis. J Ethnopharmacol. 2016;181:50–58.
2. Cha TW, Kim M, Kim M, Chae JS, Lee JH. Blood pressure-lowering effect of Korean red ginseng associated with decreased circulating Lp-PLA2 activity and lysophosphatidylcholines and increased dihydrobiopterin level in prehypertensive subjects. Hypertens Res. 2016;39:449–56.
3. Guan YY, Zhou JG, Zhang Z, Wang GL, Cai BX, Hong L et al. Ginsenoside-Rd from *Panax notoginseng* blocks Ca^{2+} influx through receptor- and store-operated Ca^{2+} channels in vascular smooth muscle cells. Eur J Pharmacol. 2006;548:129–36.
4. Lee CH, Kim JH. A review on the medicinal potentials of ginseng and ginsenosides on cardiovascular diseases. J Ginseng Res. 2014;38:161–6.
5. Liu P, Yu HS, Zhang LJ, Song XB, Kang LP, Liu JY et al. A rapid method for chemical fingerprint analysis of *Panax notoginseng* powders by ultra performance liquid chromatography coupled with quadrupole time-of-flight mass spectrometry. Chin J Nat Med. 2015;13:471–80.
6. Ma L, Xiao P. Effects of *Panax notoginseng* saponins on platelet aggregation in rats with middle cerebral artery occlusion or in vitro and on lipid fluidity of platelet membrane. Phytother Res. 1998;12:138–40.

7. Chen Z-H, Li J, Liu J, Zhao Y, Zhang P, Zhang M-X et al. Saponins isolated from the root of *Panax notoginseng* showed significant anti-diabetic effects in KK-Ay mice. Am J Chin Med. 2008;36:939–51.
8. Lee K-H, Morris-Natschke S, Qian K, Dong Y, Yang X, Zhou T et al. Recent progress of research on herbal products used in traditional Chinese medicine: the herbs belonging to the Divine Husbandman's Herbal Foundation Canon. J Tradit Complement Med. 2012;2:6–26.
9. Liu LL, Yan L, Chen YH, Zeng GH, Zhou Y, Chen HP et al. A role for diallyl trisulfide in mitochondrial antioxidative stress contributes to its protective effects against vascular endothelial impairment. Eur J Pharmacol. 2014;725:23–31.
10. Pan C, Huo Y, An X, Singh G, Chen M, Yang Z et al. *Panax notoginseng* and its components decreased hypertension via stimulation of endothelial-dependent vessel dilatation. Vasc Pharmacol. 2012;56:150–8.
11. Wang M-M, Xue M, Xu Y-G, Miao Y, Kou N, Yang L et al. *Panax notoginseng* saponin is superior to aspirin in inhibiting platelet adhesion to injured endothelial cells through COX pathway in vitro. Thromb Res. 2016;141:146–52.
12. Kang SY, Schini-Kerth VB, Kim ND. Ginsenosides of the protopanaxatriol group cause endothelium-dependent relaxation in the rat aorta. Life Sci. 1995;56:1577–86.
13. Yu J, Eto M, Akishita M, Kaneko A, Ouchi Y, Okabe T. Signaling pathway of nitric oxide production induced by ginsenoside Rb1 in human aortic endothelial cells: a possible involvement of androgen receptor. Biochem Biophys Res Commun. 2007;353:764–9.
14. Shen K, Leung SW, Ji L, Huang Y, Hou M, Xu A et al. Notoginsenoside Ft1 activates both glucocorticoid and estrogen receptors to induce endothelium-dependent, nitric oxide-mediated relaxations in rat mesenteric arteries. Biochem Pharmacol. 2014;88:66–74.
15. Cai BX, Li XY, Chen JH, Tang YB, Wang GL, Zhou JG et al. Ginsenoside-Rd, a new voltage-independent Ca^{2+} entry blocker, reverses basilar hypertrophic remodeling in stroke-prone renovascular hypertensive rats. Eur J Pharmacol. 2009;606:142–9.
16. Li J, Xie ZZ, Tang YB, Zhou JG.Guan YY, Ginsenoside-Rd, a purified component from *Panax notoginseng* saponins, prevents atherosclerosis in apoE knockout mice. Eur J Pharmacol. 652:104–10.
17. Bei L, Hu T, Qian ZM, Shen X. Extracellular Ca^{2+} regulates the respiratory burst of human neutrophils. Biochim Biophys Acta. 1998;1404:475–83.
18. Choong YK, Sun SQ, Zhou Q, Ismail Z, Rashid BAA, Tao JX. Determination of storage stability of the crude extracts of *Ganoderma lucidum* using FTIR and 2D-IR spectroscopy. Vib Spectrosc. 2011;57:87–96.
19. Li H, Hong da H, Son YK, Na SH, Jung WK, Bae YM et al. Cilostazol induces vasodilation through the activation of Ca^{2+}-activated K^{+} channels in aortic smooth muscle. Vasc Pharmacol. 2015;70:15–22.
20. Geissler M, Oellig C, Moss K, Schwack W, Henkel M, Hausmann R. High-performance thin-layer chromatography (HPTLC) for the simultaneous quantification of the cyclic lipopeptides Surfactin, Iturin A and Fengycin in culture samples of *Bacillus* species. J Chromatogr B Anal Technol Biomed Life Sci. 2017;1044-1045:214–24.
21. Wagner H, Bauer R, Melchart D, Xiao PG, Staudinger A Chromatographic Fingerprint Analysis of Herbal Medicines Volume III: Thin-layer and High Performance Liquid Chromatography of Chinese Drugs: Springer International Publishing, New York City, United States; 2014;267.
22. Ameer OZ, Salman IM, Siddiqui MJ, Yam MF, Sriramaneni RN, Mohamed AJ et al. Pharmacological mechanisms underlying the vascular activities of *Loranthus ferrugineus* Roxb. in rat thoracic aorta. J Ethnopharmacol. 2010;127:19–25.
23. Loh YC, Tan CS, Ch'ng YS, Ahmad M, Asmawi MZ, Yam MF. Overview of antagonists used for determining the mechanisms of action employed by potential vasodilators with their suggested signaling pathways. Molecules. 2016;21:495.
24. Senejoux F, Demougeot C, Cuciureanu M, Miron A, Cuciureanu R, Berthelot A et al. Vasorelaxant effects and mechanisms of action of *Heracleum sphondylium* L. (Apiaceae) in rat thoracic aorta. J Ethnopharmacol. 2013;147:536–9.
25. Tan CS, Ch'ng YS, Loh YC, Asmawi MZ, Ahmad M, Yam MF. Vasorelaxation effect of *Glycyrrhizae uralensis* through the endothelium-dependent pathway. J Ethnopharmacol. 2017;199:149–60.
26. Sun SQ, Zhou Q, Qin Z Atlas of Two-dimensional Correlation Infrared Spectroscopy for Traditional Chinese Medicine Identification: Chemical Industry Press, Beijing; 2003;2:1–358.
27. Sun S, Zhou Q, Chen J *Analysis of Traditional Chinese Medicine by Infrared Spectroscopy*: Chemical Industry Press, Beijing; 2010;36–69.
28. Ch'ng YS, Tan CS, Loh YC, Ahmad M, Asmawi MZ, Yam MF. Vasorelaxation Study and Tri-Step Infrared Spectroscopy Analysis of Malaysian Local Herbs. J Pharmacopunct. 2016;19:145.
29. Leung KW, Wong AS. Pharmacology of ginsenosides: a literature review. Chin Med. 2010;5:20.
30. Li L, Yang HG, Yuan TY, Zhao Y, Du GH. Rho kinase inhibition activity of pinocembrin in rat aortic rings contracted by angiotensin II. Chin J Nat Med. 2013;11:258–63.
31. Rameshrad M, Babaei H, Azarmi Y, Fouladia DF. Rat aorta as a pharmacological tool for in vitro and in vivo studies. Life Sci. 2016;145:190–204.
32. Ignarro LJ. Biological actions and properties of endothelium-derived nitric oxide formed and released from artery and vein. Circ Res. 1989;65:1–21.
33. Moncada S. A2. Nitric oxide and bioenergetics: physiology and pathophysiology. Nitric Oxide. 2007;17:9.
34. Vanhoutte PM. Endothelium-derived relaxing and contracting factors. Adv Nephrol Necker Hosp. 1990;19:3–16.
35. Mayer B, Brunner F, Schmidt K. Inhibition of nitric oxide synthesis by methylene blue. Biochem Pharmacol. 1993;45:367–74.
36. Olson LJ, Knych ET Jr., Herzig TC, Drewett JG. Selective guanylyl cyclase inhibitor reverses nitric oxide-induced vasorelaxation. Hypertension. 1997;29:254–61.
37. Berumen LC, Rodriguez A, Miledi R, Garcia-Alcocer G. Serotonin receptors in hippocampus. Sci World J. 2012;2012:823493.
38. Jakala P, Pere E, Lehtinen R, Turpeinen A, Korpela R, Vapaatalo H. Cardiovascular activity of milk casein-derived tripeptides and plant sterols in spontaneously hypertensive rats. J Physiol Pharmacol. 2009;60:11–20.
39. Yildiz O, Gul H, Seyrek M. Pharmacology of Arterial Grafts for Coronary Artery Bypass Surgery: INTECH Open Access Publisher, Croatia; 2013;251–76.
40. Feletou M, Vanhoutte P. *EDHF: The Complete Story*: 1st edition, CRC Press, Boca Raton, FL, USA; 2005;1–173.
41. Luksha L, Agewall S, Kublickiene K. Endothelium-derived hyperpolarizing factor in vascular physiology and cardiovascular disease. Atherosclerosis. 2009;202:330–44.
42. Marchenko SM, Sage SO. Electrical properties of resting and acetylcholine-stimulated endothelium in intact rat aorta. J Physiol. 1993;462:735–51.